2026 IEEE International Conference on Robotics and Automation (ICRA 2026)
June 1-5, 2026. Vienna, Austria

Proactive Grasp Assistance in a Robotic Hand Exoskeleton Improves Performance and Preference in Challenging Tasks

Benjamin Davis, Emily Huynh, and Hannah S. Stuart*

Abstract— **Advancements in perception, planning, and control enable the development of wearable robots capable of proactively assisting users in avoiding potentially negative outcomes. However, the introduction of robotic assistance in general is often associated with a loss in the sense of agency, a factor traditionally associated with overall device acceptance. Recent work provides a different perspective, showing that contextual proactive assistance is well-received for teleoperation or shared workspace tasks. Still, no works have investigated the impact of proactive assistance for wearable grasping devices, where physical interactions have increased potential for disrupting the user's experience. In this study, we analyze the impact of proactive assistance in a hand exoskeleton with an abstracted grasping task of varying difficulty. We show that in general, the presence of assistance does not significantly reduce experience or the sense of agency. In fact, in a difficult task, subjects strongly prefer proactive assistance, likely as a result of its provided utility. When the task is easily completed without assistance, subjects indicate no strong preference for assisted conditions. Our results challenge the notion of a direct trade-off between robotic assistance and agency, suggesting that well-designed assistance can improve performance and user preference without compromising their sense of control.**

I. INTRODUCTION

In the evolving landscape of assistive robotics, researchers are exploring proactive systems that anticipate and mitigate challenges as they arise. This proactive assistance, where a robot intervenes without user initiation based on internal predictions, holds promise for enhanced safety and performance. Recent work on such proactive assistance can be found across various assistive technologies, such as wheelchairs with active obstacle avoidance [1], [2], lower-limb exoskeletons that prevent tripping and falling [3], [4], [5], or hand exoskeletons that adjust their grasp to prevent slip [6]. Grasp assistance presents a compelling use case for proactive robot intervention, with potential to restore grasp reflexes for individuals with stroke or spinal cord injury [7], [8] or users of augmentative exoskeletons like the NASA/GM Robo-Glove [9]. In either case, proactive grasp assistance could prevent users from accidentally dropping objects, over-grasping, or attempting harmful grasps.

While proactive assistance may have important benefits for grasping and is increasingly achievable through advancements in sensing, intent detection algorithms, and adaptive control strategies (e.g. [10], [11], [12]), its integration into an exoskeleton may reduce the user experience. Studies show that robotic assistance reduces the sense of agency, or feeling of being in control of one's own actions and outcomes [13], [14]. Users generally prefer to maintain this sense over systems they operate [15], with positive links between agency and task motivation [16], perceived personal responsibility [17], and situational responsiveness [18], [19]. The sense of agency is particularly important to improving long-term acceptance and effectiveness of assistive technologies [20]. A study on user preference of different levels of automation in the context of assistive technology supports the importance of agency for the user experience, with users preferring lower levels of robotic assistance [21]. However, the sense of agency is not well explored in the context of robotic exoskeletons, even though its importance is acknowledged [22], [23]. Additionally, the robotic assistance supplied in prior work on agency and assistance [13], [14], [21] reduces user burden by guiding precise movements and automating low-level tasks, which does not fit our definition of proactive.

The effect of **proactive** robotic assistance on the user experience, including the sense of agency, is not yet a matter of consensus. Some studies in non-assistive human-robot interaction (e.g. teleoperation or shared workspace tasks) show that users appreciate proactive assistance [24], [25], [26], while others propose that user preference depends on factors like the aggressiveness of assistance, task difficulty, and the user's own internal motivations and expectations [27], [28], [29]. For hand exoskeletons and other platforms for physical human-robot interactions, the effects of these factors are not well understood. We seek to provide insight on these relationships in this work.

Establishing these relationships could inform discrete task-level assistive control policy designs, but the development of adaptive control policies requires an online, real-time proxy for agency and user experience. Collier et al. [30] propose the angle of disagreement between the user input and robot motion as an online proxy metric for agency in a teleoperation task. For exoskeletons, where the motion of the user and robot cannot disagree due to physical coupling, interaction forces present a promising proxy metric instead. Some existing work has presented interaction forces alongside user experience scores, yet their relationship with each other has yet to be explored [31].

To address these gaps, we present a study that examines the effect of proactive assistance on performance and user experience metrics in a robotic hand exoskeleton. We explore how user preference and agency are affected by different levels of robot aggressiveness and task difficulty, inspired by previous work [27]. We also measure interaction forces

B. Davis, E. Huynh, and H.S. Stuart are with the Embodied Dexterity Group, Dept. of Mechanical Engineering, University of California Berkeley, Berkeley, CA, USA.

* Corresponding author email: hstuart@berkeley.edu

There is a video supplement associated with this work.

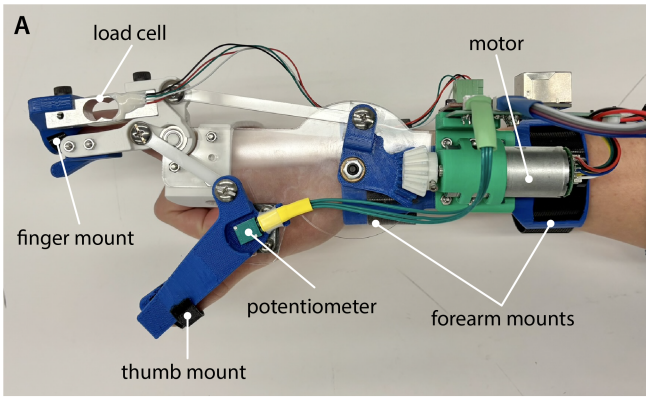

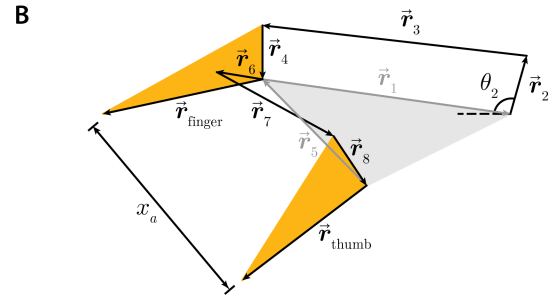

Fig. 1. (A) depicts the worn hand exoskeleton mounted at the forearm, thumb, and index finger with Velcro straps. (B) shows the system of linkages that generate grasping motion. Colored shapes denote rigid bodies. The yellow triangles represent the thumb and finger links, while the grey body and arrows represent ground links.

between the user and exoskeleton to observe its usefulness as a real-time proxy metric for agency. In Section II, we describe our hand exoskeleton hardware and controller before explaining the task, proactive assistance design, procedure, metrics, and statistical analysis methods in Section III. The results of our study are presented in Section IV, followed by a discussion of key takeaways in Section V. Finally, we present our conclusions in Section VI.

II. Hand Exoskeleton Design and Control

A. Implementation

Our hand exoskeleton, shown in Fig. 1A, is a two-finger, one-degree-of-freedom investigational device derived from the Motor-Augmented Wrist-Driven Orthosis [32] for grasp augmentation. The exoskeleton is mounted to the user's forearm, index finger, and thumb with Velcro straps. It is actuated by a 12V brushed DC motor with encoder (Pololu) that drives the coupled motion of the thumb and index finger through a series of two four-bar linkages (Fig. 1B). Since the encoder is relative, a potentiometer (Alps Alpine) in the thumb is used to calibrate its absolute position. A 5kg load cell (SparkFun) measures the interaction force between the user's index finger and the exoskeleton. A separate load cell to measure thumb interaction forces was deemed redundant during initial device development due to coupled motion of the thumb and index finger.

The exoskeleton's grasp state can be defined by its grasp aperture x_a, or distance between the thumb and finger components. To obtain grasp aperture from motor encoder readings, we first determine the configuration of the first four-bar linkage ($\vec{r}_1, \vec{r}_2, \vec{r}_3, \vec{r}_4$) using the vector loop method:

$$\vec{r}_1 + \vec{r}_2 + \vec{r}_3 + \vec{r}_4 = 0. \tag{1}$$

Through Euler's formula, this can be broken down into real and imaginary components:

$$r_1 \cos\theta_1 + r_2 \cos\theta_2 + r_3 \cos\theta_3 + r_4 \cos\theta_4 = 0 \tag{2}$$

$$r_1 \sin\theta_1 + r_2 \sin\theta_2 + r_3 \sin\theta_3 + r_4 \sin\theta_4 = 0 \tag{3}$$

where $\vec{r}_1$ is a vector with magnitude r_1 and angle θ_1, $\vec{r}_2$ is a vector with magnitude r_2 and angle θ_2, and so on. Since the ground link angle θ_1 and input link angle θ_2 are known, equations (2) and (3) can be solved to provide the full linkage configuration. This process is repeated to solve for the configuration of the second four-bar linkage with vectors $\vec{r}_5, \vec{r}_6, \vec{r}_7$, and $\vec{r}_8$. The input link $\vec{r}_6$ has constant relative position to $\vec{r}_4$, and the ground link $\vec{r}_5$ is known. Once all link positions have been calculated, the grasp aperture can be found:

$$x_a = ||\vec{r}_{finger} - (\vec{r}_{thumb} - \vec{r}_5)||. \tag{4}$$

For our device, x_a is nearly linear with respect to the input angle θ_2. Therefore, we linearly approximate the linkage kinematics and use θ_2 to represent grasp aperture. Angle θ_2 can be determined through a scaling and offset of the encoder value x_{enc} based on encoder counts per rotation N_{CPR} and bevel gear ratio R:

$$\theta_2 = 90 - 360\frac{x_{enc}}{N_{CPR}R}. \tag{5}$$

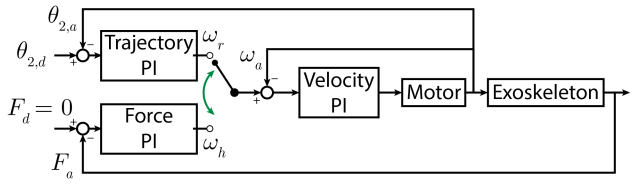

Fig. 2. The cascaded controller of the exoskeleton can switch between two outer controllers, both of which generate angular velocity commands for a low-level Velocity PI controller to follow. The Force PI controller follows the user's movements by minimizing the interaction force F_a, while the Trajectory PI controller follows a trajectory $\theta_{2,d}$ to guide the user.

B. Control

The exoskeleton is operated by the cascaded PI controller shown in Fig. 2. The outer PI loop operates at 50 Hz and can switch between a Force PI controller and Trajectory PI controller. The Force PI controller follows the user's motion by minimizing the actual interaction force F_a (i.e. force setpoint $F_d = 0$), generating human-led velocity commands ω_h. The Trajectory PI controller tracks a desired input angle $\theta_{2,d}$ (representing grasp aperture x_a) and outputs robot-led velocity commands ω_r. The commands from the selected controller are fed to an incremental Velocity PI controller that regulates motor PWM at 300 Hz.

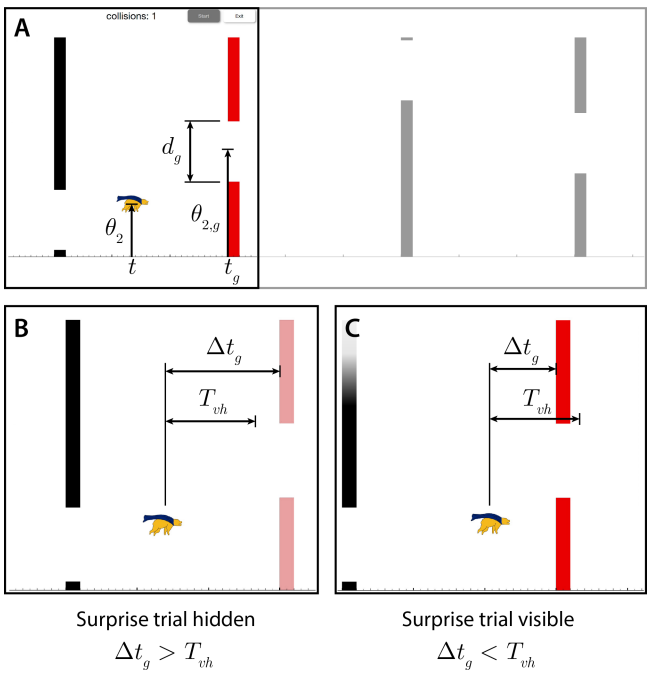

Fig. 3. (A) The user controls the altitude of a flying golden bear in a constant-speed side-scrolling game by adjusting their grasp aperture, represented by θ_2. They must navigate through stationary gates described by their time of occurrence t_g, height $\theta_{2,g}$, and gap distance d_g. The black boxed region shows the visible portion of the GUI. Future trials are outlined in gray for visualization purposes. Red gates represent surprise trials, while black gates represent default trials. (B,C) The red surprise gate remains hidden until its distance from the bear Δt_g decreases below some visible horizon T_{vh}.

III. EXPERIMENTAL METHODS

A. Participants

The results are based on data from 18 participants (10 male, 8 female) with an average age of 23.8 (SD: 4.7). One participant was left-handed, and no participants reported limb differences or impairments to hand function. The participant pool consists of individuals from the university student population and surrounding community. The experimental protocol is approved by the University of California, Berkeley Institutional Review Board (IRB) under protocol #2024-11-17990.

B. Task

The user's main task is to navigate a flying golden bear through gates displayed on a graphical user interface (GUI), shown in Fig. 3. The bear's horizontal position represents the current time t, and its altitude depicts grasp aperture θ_2. The GUI window is centered on the current time, meaning the bear remains centered on the screen. This window has a width of two seconds, meaning users can see one second in the future (to the bear's right) and one second in the past (to the bear's left). Gates are placed every 1.5 seconds and described by time t_g, height $\theta_{2,g}$, and gap distance d_g (see Fig. 3A). Each gate marks a new trial and is considered successful if the user succeeds in avoiding a collision.

The task includes two types of trials: surprise trials—indicated by red gates—and default trials—marked by black gates. Surprise trials, which occur every third trial, remain hidden until its distance from the user Δt_g falls below a specified visible horizon (T_{vh}), as indicated in Fig. 3B,C. The difficulty of the task can be altered by changing T_{vh}. Default trials are unaffected by the visible horizon, meaning they are always visible within the window.

C. Proactive Assistance

By default, the hand exoskeleton operates in its force-controlled mode to provide the user with control. Proactive assistance can be applied during the task by switching the exoskeleton to trajectory-following mode. The outer loop controller follows a linear trajectory to the center of the gate $\theta_{2,g}$ defined by velocity $\omega_{2,assist} = 45°/\text{sec}$.

The point at which this switch occurs during a trial, which determines the aggressiveness of assistance, is triggered based on the estimated probability of success P_s. When P_s drops below a success probability threshold $P_{s,th}$, the mode is switched. We estimate P_s with a multivariable logistic regression model with five input features. First, we extract these features at each timestep k. The selected features include the time until the next gate $\Delta t_g(k)$, absolute distance in θ_2 between the user and the gate $|\Delta\theta_{2,g}(k)|$, user velocity relative to the direction of the gate $\tilde{\omega}_2(k)$, minimum absolute velocity required to reach the gate $|\omega_{2,min}(k)|$, and rate of change of this minimum velocity $\dot{\omega}_{2,min}(k)$. The features are defined as follows:

$$\begin{aligned}
\Delta t_g(k) &= t_g - t(k) \\
|\Delta\theta_{2,g}(k)| &= |\theta_{2,g} - \theta_2(k)| \\
\tilde{\omega}_2(k) &= \omega_2(k)\text{sign}(\Delta\theta_{2,g}(k)) \\
|\omega_{2,min}(k)| &= \frac{|\Delta\theta_{2,g}(k)|}{\Delta t_g(k)} \\
\dot{\omega}_{2,min}(k) &= \frac{|\omega_{2,min}(k)| - |\omega_{2,min}(k-1)|}{t(k) - t(k-1)}
\end{aligned}$$

where $\omega_2(k)$ is the discrete time velocity approximation of the user's position $\theta_2(k)$.

After feature extraction, we filter our data based on two criteria. First, only data points where $\Delta t_g(k) < 1$ are included. The GUI window only allows the user to see one second ahead, meaning points where $\Delta t_g(k) > 1$ are less likely to relate to the trial outcome. Second, we filter out data where the bear is within the gate opening, i.e. $|\Delta\theta_{2,g}(k)| < \frac{d_g}{2}$. This is because the user can perform any movements within this range and still succeed, so meaningful patterns are less likely to emerge or be consistent with larger trends. Both of these steps benefited model performance during pilot testing. After filtering, the model is trained on standardized features. The model achieves a mean cross-validated F1 score of 0.75 (SD: 0.036) across 18 participants on the training round data.

D. Experimental Procedure

To begin, the subject sits at a desk and faces a laptop. They don the hand exoskeleton on their right hand, tightening the Velcro straps as necessary to ensure a secure fit.

The subject then completes an introductory round and a training round. The introductory round consists of 40 trials with the purpose of getting familiar with the device and task. Every third trial is a surprise trial, accounting for 13 trials in total. The training round, used to collect data for training the success prediction model, consists of 100 consecutive surprise trials. No proactive assistance is provided in either round. For both rounds, each surprise trial has a randomly sampled visible horizon $T_{vh} \sim U(0.33, 1)$ and gate height $\theta_{2,g} \sim U(68°, 84°)$, and a set gap distance $d_g = 6°$. The visible horizon range helps provide a balanced dataset of successful and failed trials. The gate height range represents grasp apertures within a comfortable range of motion.

Once the training round is completed and the success prediction model is trained, the subject begins rounds for the experimental conditions. The subject encounters six different conditions composed of two levels of round difficulty and three assistance modes based on aggressiveness. We control round difficulty with the visible horizon T_{vh}. We select a visible horizon of $T_{vh} = 1.0$ seconds to represent an "easy" task, and a visible horizon of $T_{vh} = 0.4$ seconds to represent a "hard" task. The hard task visible horizon is just longer than human reaction times to visual stimuli (0.2-0.3 seconds) [33] and was found experimentally to be difficult but not impossible. Robot aggressiveness is determined by the success probability threshold $P_{s,th}$, where assistance is triggered when the model predicted success probability drops below this threshold, $P_s < P_{s,th}$. Three success probability thresholds form the three assistance modes based on aggressiveness: no assistance ($P_{s,th} = 0$), "timid" ($P_{s,th} = 0.2$), and "aggressive" ($P_{s,th} = 0.6$). The order of conditions is counterbalanced using a Latin square design to control for learning and fatigue effects. Each row is duplicated twice and their order is randomized to accommodate 18 participants.

For each condition, the subject completes a warm-up round of 20 trials, followed by two recorded rounds of 80 trials each with breaks in between. All experimental rounds include surprise trials every third trial, totaling 6 surprise trials in the warm-up round and 26 in each recorded round. In the warm-up, trial heights are generated randomly. The two 80-trial rounds randomly select from two pre-generated trial height sequences without replacement. These two pre-generated sequences are used across all conditions and all subjects to prevent discrepancies in difficulty across rounds. Pilot testing showed that memorization of these sequences to any significant degree is unlikely, especially with the presence of breaks and survey questions. The warm-up data is ignored, resulting in data from 160 trials (52 surprise) per condition. After all three rounds for a condition are completed, the subject answers a set of survey questions detailed in Section III-E.

E. Metrics

1) Objective Metrics: We assess subject performance by recording trial success rates for default trials $R_{s,d}$ and surprise trials $R_{s,s}$ within each condition. For surprise trials, we also collect assist utilization rate R_{au}, or percentage of surprise trials where P_s drops below $P_{s,th}$ and proactive assistance is triggered. From the exoskeleton hardware, we measure the average absolute interaction force F_{int} between the index finger and exoskeleton for each surprise trial.

2) Subjective Metrics: A set of survey questions assesses the subject's experience with the device for each condition. Due to the unchanging nature of the default trials across conditions, the survey questions are asked specifically regarding the surprise trials. Three 7-point Likert questions measure the subject's subjective sense of **agency**, the perceived **helpfulness** of the robot, their overall **preference** towards the condition. We also measure the subject's perceived workload with the unweighted NASA TLX questionnaire [34]. Data is collected for all six TLX questions on 21-point scales (0-100, increments of 5), but we only perform statistical analysis on the average score. Our full survey can be found in the Appendix.

F. Statistical Analysis

We evaluate the effects of task difficulty and assistance mode (aggressiveness) using appropriate statistical tests for each metric. For success rates $R_{s,d}$ and $R_{s,s}$ and assistance utilization rate R_{au}, we use binomial generalized linear mixed models (GLMMs) due to their bounded nature. Average interaction force F_{int} is continuous and bounded by zero, so we use a Gamma GLMM. For subjective data, we approximate the NASA TLX score as continuous due to its large number of bins and analyze it with a linear mixed-effects model (LME). Agency, helpfulness, and preference are ordinal data, and we evaluate them using non-parametric Friedman tests. To control for learning and fatigue, we include condition order as a covariate when allowed by the model framework (i.e., for the GLMMs and LME).

For the parametric models (GLMMs and LME), we use χ^2 likelihood ratio tests to determine the significance of main effects. When possible, we fit one model to the data, including task difficulty and assistance mode as main effects, as well as their interaction. If an interaction effect between task difficulty and assistance is present, we conduct separate pairwise comparisons for each level of difficulty. If the main effect of assistance is significant but the interaction is not, we conduct a single set of pairwise comparisons across assistance modes. If the single model fails to converge, we fit separate models to each level of difficulty and proceed with separate pairwise comparisons. For pairwise comparisons, we provide estimated difference Δ and p-value, correcting for family-wise error rate with Tukey's Honestly Significant Difference test. For the ordinal survey data, we perform separate Friedman tests for each level of difficulty, followed by post-hoc pairwise Wilcoxon signed-rank tests to identify specific differences. We adjust p-values for these comparisons using the Holm-Bonferroni correction.

We note one deviation from this approach. Assistance utilization rate is deterministically zero for the no assistance condition, so we exclude it from the model to avoid issues of complete separation. As such, we test for significance between this assistance mode and the others by checking

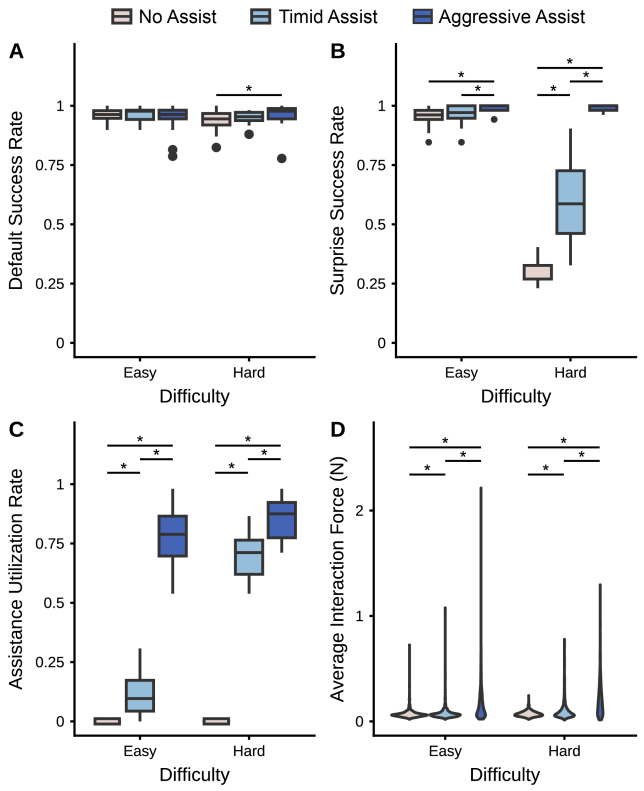

Fig. 4. Results for default trial success rate per condition (A), surprise trial success rate per condition (B), assist utilization rate per condition (C), and average interaction force per trial (D). Significant comparisons are made between estimated marginal means and denoted with horizontal lines with asterisks. In (C), significant comparisons with the No Assist condition represent a 95% confidence interval for the difference between groups not containing 0. For the rest of the comparisons, significance is determined by the threshold $p < 0.05$.

whether the confidence interval of the estimated marginal mean excludes zero.

All analysis is performed with R v4.5.1. Linear mixed modeling is completed with the "nlme" package [35], and generalized linear mixed modeling is completed with the "lme4" package [36]. Estimated marginal means are calculated with the "emmeans" package [37].

IV. RESULTS

A. Objective Metrics

Default trial success rate is close to perfect for every condition (Fig. 4A). We analyze the two difficulty levels separately due to a strong ceiling effect in the easy task. This also prevents model convergence for the easy task, precluding formal analysis of trends and pairwise comparisons. For the hard task, the model converges, revealing a significant effect of assistance mode on default success rate ($\chi^2(2) = 8.2,\ p = 0.017$). Pairwise tests indicate that subjects perform better in default trials with aggressive (A) assistance compared to the unassisted (U) mode (U-A: $\Delta = -0.018,\ p = 0.018$), even though assistance does not occur during default trials. The effect of condition order is not significant ($\chi^2(5) = 8.8,\ p = 0.12$).

Surprise trial success rate remains close to perfect for the easy task, but performance drops for the no assistance and timid conditions in the hard task (Fig. 4B). The two difficulty levels are analyzed separately for surprise trial success rate, again due to ceiling effects. Assistance mode has a significant effect on surprise success rate for both difficulties (easy: $\chi^2(2) = 21,\ p < 0.0001$; hard: $\chi^2(2) = 1198,\ p < 0.0001$). In the easy task, aggressive assistance improves success rate over timid (T) assistance (T-A: $\Delta = -0.020,\ p = 0.013$) and no assistance (U-A: $\Delta = -0.0267,\ p = 0.0039$). In the hard task, timid assistance increases success compared to no assistance (U-T: $\Delta = -0.30,\ p < 0.0001$), and aggressive assistance increases success compared to timid assistance (T-A: $\Delta = -0.38,\ p < 0.0001$) and no assistance (U-A: $\Delta = -0.69,\ p < 0.0001$). Condition order has significant effects in the hard task ($\chi^2(5) = 29,\ p < 0.0001$) but not in the easy task ($\chi^2(5) = 8.8,\ p = 0.12$).

Assistance is utilized more frequently with increasing task difficulty and robot aggressiveness (Fig. 4C). The interaction between assistance mode and task difficulty is significant ($\chi^2(6) = 210,\ p < 0.0001$). For the easy task, assistance utilization is significantly greater than zero for the timid mode (U-T: pred. rate $= 0.11$, 95% CI $[0.082, 0.15]$) and aggressive mode (U-A: pred. rate $= 0.80$, 95% CI $[0.75, 0.84]$). The same is true for the difficult task (U-T: pred. rate $= 0.71$, 95% CI $[0.65, 0.76]$; U-A: pred. rate $= 0.87$, 95% CI $[0.83, 0.90]$). The aggressive mode sees higher utilization than the timid mode across the easy task (T-A: $\Delta = -0.68,\ p < 0.0001$) and hard task (T-A: $\Delta = -0.16,\ p < 0.0001$). The effect of condition order is significant ($\chi^2(20) = 51,\ p = 0.00015$).

The average interaction force per trial (Fig. 4D) is also affected by both task difficulty and assistance mode, as indicated by a significant interaction effect between them ($\chi^2(2) = 63,\ p < 0.0001$). Average forces for the timid mode are larger than those experienced without assistance across both levels of difficulty (U-T, easy: $\Delta = -0.0051,\ p = 0.0060$; U-T, hard: $\Delta = -0.025,\ p < 0.0001$). The aggressive mode induces larger interaction forces than the timid mode (T-A, easy: $\Delta = -0.081,\ p < 0.0001$; T-A, hard: $\Delta = -0.10,\ p < 0.0001$) and no assistance mode (U-A, easy: $\Delta = -0.086,\ p < 0.0001$; U-A, hard: $\Delta = -0.13,\ p < 0.0001$) for both difficulties. A significant effect of condition order on average interaction force is present ($\chi^2(5) = 45,\ p < 0.0001$).

B. Subjective Metrics

Assistance mode has a significant effect on agency (Fig. 5A) in the hard task ($\chi^2(2) = 12.32,\ p = 0.0021$) but not in the easy task ($\chi^2(2) = 2.1,\ p = 0.35$). A strong majority of participants report positive agency scores in the easy task, but this number decreases when the difficulty is increased. Agency appears to be higher without assistance in the hard task, although pairwise tests are not significant (N-T: $r = 0.52,\ p = 0.10$, N-A: $r = 0.55,\ p = 0.10$).

Subjects perceive the robot as more helpful with increasing robot aggressiveness, as shown in Fig. 5B, with the effect being significant for both levels of difficulty (easy: $\chi^2(2) =$

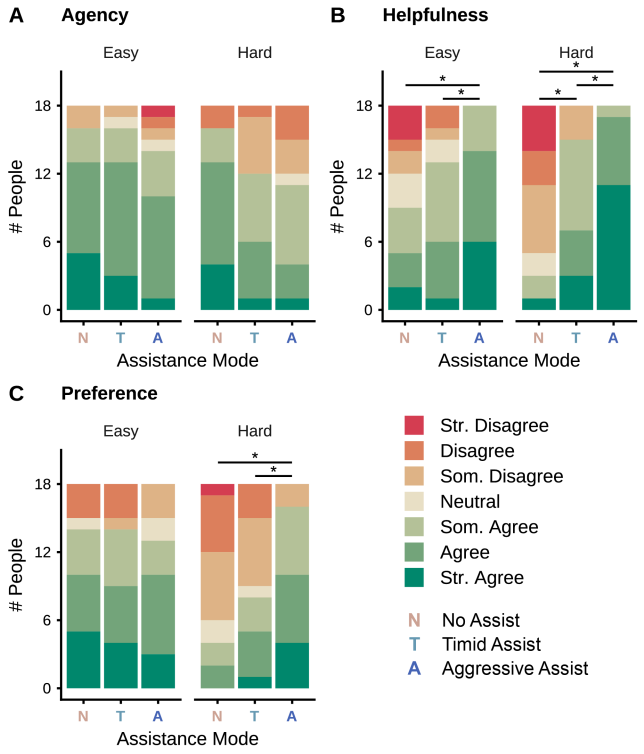

Fig. 5. Likert-scale survey results for agency (A), helpfulness (B), and preference (C). Significant comparisons are made between estimated marginal means and denoted with horizontal lines with asterisks. Significance is determined by the threshold $p < 0.05$.

15, $p = 0.00052$; hard: $\chi^2(2) = 23$, $p < 0.0001$). Pairwise tests for the easy condition reveal significant differences between aggressive assistance and both other modes (N-A: $r = 0.76$, $p = 0.0097$; T-A: $r = 0.73$, $p = 0.0097$). In the hard condition, every comparison is statistically significant (N-T: $r = 0.73$, $p = 0.0097$; N-A: $r = 0.87$, $p = 0.0014$; T-A: $r = 0.76$, $p = 0.0097$), indicating that subjects perceive timid assistance as more helpful than no assistance but not as helpful as the aggressive mode.

Results in Fig. 5C show that there is no clear assistance mode preference in the easy condition ($\chi^2(2) = 0.27$, $p = 0.87$), but preferences are significantly different in the hard condition ($\chi^2(2) = 11$, $p = 0.0046$). Follow-up pairwise tests for the hard task show that subjects have no significant preference between the unassisted and timid modes (U-T: $r = 0.34$, $p = 0.14$), and the aggressive mode is preferred over both (U-A: $r = 0.69$, $p = 0.011$; T-A: $r = 0.60$, $p = 0.026$).

Average NASA TLX scores, as well as scores for individual metrics, are shown in Fig. 6. The effect of assistance mode changes significantly with task difficulty ($\chi^2(2) = 23$, $p < 0.0001$). No difference in perceived workload is present for the easy task, but aggressive assistance decreases workload compared to the timid and unassisted modes for the hard task (U-A: $\Delta = 27$, $p < 0.0001$; T-A: $\Delta = 19$, $p = 0.0001$). The timid mode may slightly reduce workload compared to no assistance, although this is not significant ($\Delta = 8.1$, $p = 0.13$). These trends are visually similar across individual TLX metrics, but we do not include a formal statistical analysis of each one.

V. DISCUSSION

Our results indicate that the effects of proactive assistance depend strongly on the robot's aggressiveness and task difficulty. In easy tasks, proactive assistance provides negligible benefit to the user's performance or experience. Conversely, in challenging tasks, users strongly prefer the most aggressive assistance mode, which improves performance and reduces perceived workload.

These outcomes suggest that user preference is driven by the actual utility of assistance. In easy tasks, both timid and aggressive assistance modes are perceived as helpful and see high usage, but neither improves success or workload, leading to no change in user preference. In hard tasks, aggressive assistance provides utility through significant improvements to success and workload, leading to higher user preference scores. These results align with prior work in non-physical human-robot interaction [27], suggesting that the introduction of interaction forces may not be harmful to the user experience on its own. Our results support this, showing that users do not give less preference to conditions with higher average interaction forces.

Predictably, the average interaction force increases with aggressiveness as the robot physically corrects the user, but it lacks correlation with the reported sense of agency. In fact, a majority of users report feeling some level of control over the device across all conditions, although a reduction in agency due to proactive assistance is almost significant for the hard task. This suggests that brief, goal-aligned proactive robot interjections do not strongly reduce agency, adding nuance to the idea that automation inherently reduces it [13]. We propose that this occurs due to differences in the form of assistance. The forms of assistance discussed in [13] automate varying degrees of low-level control over the course of the whole task. In our case, the assistance briefly takes control to guide the user toward success, before and after which the user has full control of the device. These actions may not be jarring enough to reduce the user's general sense of control. Furthermore, the increase in interaction force observed with increasing levels of assistance is not mirrored by significant reductions in agency, showing that interaction force does not serve as an accurate real-time proxy metric for agency in this scenario.

Interestingly, we find that the aggressive mode of assistance provides small but significant improvements to performance in the default (unassisted) trials during the hard condition. We originally hypothesized that default success rates may decrease in assisted conditions if users develop a reliance on assistance, or their focus is disrupted by the switching of modes. However, this result suggests that there may be a psychological "carry-over" effect, where improved success from assistance in the surprise trials boosts the user's confidence, engagement, and performance in subsequent default trials. That said, the magnitude of this finding is

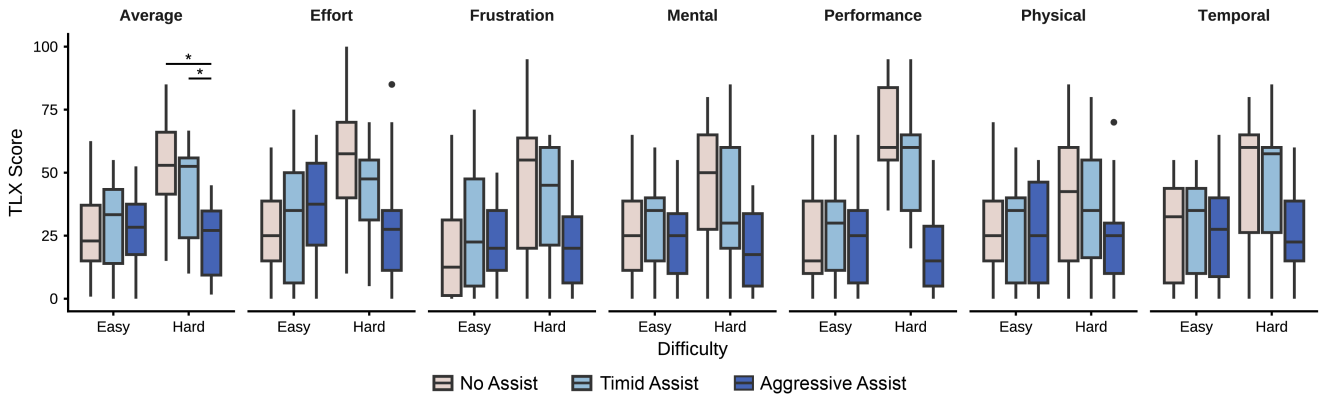

Fig. 6. The average NASA TLX score, as well as all six individual scores, are shown. Statistical analysis is only performed on the average score.

small, so we limit any definitive claims on the presence of such an effect and leave further investigation to future work.

A. Limitations and Future Work

This study was conducted with a cohort of primarily university-aged individuals in a controlled environment. The study also most closely imitates grasp augmentation for the normative population, rather than grasp assistance for users with stroke or spinal cord injuries. The generalization of our findings to different age groups and non-normative populations requires further study with a larger subject pool. The designed task, while involving a real grasping motion, is a gamified abstraction with a different objective (control the bear vs. grasp an object) that may not capture the relative priorities of success and control in real-life exoskeleton use cases. Future work should investigate the effects of proactive assistance in more applied, realistic settings. In the task, we only focus on the effects of the physical interactions themselves and ignore the potential for errant robotic assistance. Robot errors have significant impacts on user experience [27], and their effects should be investigated in future work. The use of a logistic regression model for success prediction provides sufficient distinction between our two levels of aggressiveness, as indicated by the surprise success rates and assistance utilization rates. However, this model is inherently limited in the trends it can capture compared to more advanced prediction models like long short-term memory networks (LSTMs) or Hidden Markov Models (HMMs), which could be applied in future work.

VI. CONCLUSION

In this study, we demonstrate that users strongly prefer proactive grasp assistance in a robotic hand exoskeleton when delivered in a context where its benefit is clear. The presence of such assistance appears to have a negligible effect on the sense of agency, implying that proactive assistance and its associated increases in interaction force are not inherently disruptive to the user's overall sense of control. These results also suggest that interaction force may not serve as a reliable lone proxy metric for agency, and additional metrics should be explored. Furthermore, user preference derives primarily from the actual utility of the assistance, aligning more closely with improvements in performance and workload than with perceived agency or helpfulness. While further work is needed to evaluate these effects beyond an abstracted task to real grasping scenarios for assistive device end-users, our results challenge the notion of a direct trade-off between robotic autonomy and user experience established in prior literature. Instead, they suggest that the most preferred exoskeleton solutions may be those that incorporate intelligent, context-aware assistance policies that intervene in the right moments.

APPENDIX

A. Post-Condition Survey

1. (Agency) I was in control of the device. 2. (Helpfulness) The exoskeleton helped me complete the task. 3. (Preference) I liked this condition for completing the task. 4. (TLX-mental) How mentally demanding was the task? 5. (TLX-physical) How physically demanding was the task? 6. (TLX-temporal) How hurried or rushed was the pace of the task? 7. (TLX-performance) How successful were you in accomplishing what you were asked to do? 8. (TLX-effort) How hard did you have to work to accomplish your level of performance? 9. (TLX-frustration) How insecure, discouraged, irritated, stressed, and annoyed were you?

ACKNOWLEDGMENT

This material is based upon work supported by the National Science Foundation CAREER Program under Grant No. 2237843, the National Science Foundation Graduate Research Fellowship under Grant No. 2146752. Any opinions, findings, and conclusions or recommendations expressed in this material are those of the author(s) and do not necessarily reflect the views of the National Science Foundation. The authors acknowledge the support of the members of the Embodied Dexterity Group.

REFERENCES

[1] A. Ruíz-Serrano, M. C. Reyes-Fernández, R. Posada-Gómez, A. Martínez-Sibaja, and A. A. Aguilar-Lasserre, "Obstacle avoidance embedded system for a smart wheelchair with a multimodal navigation interface," in *2014 11th International Conference on Electrical Engineering, Computing Science and Automatic Control (CCE)*, pp. 1–6, Sept. 2014.

[2] E. Erturk, S. Kim, and D. Lee, "Driving Assistance System with Obstacle Avoidance for Electric Wheelchairs," *Sensors*, vol. 24, p. 4644, Jan. 2024. Number: 14 Publisher: Multidisciplinary Digital Publishing Institute.

[3] Z. Zhang, G. Liu, T. Zheng, H. Li, S. Zhao, J. Zhao, and Y. Zhu, "Blending control method of lower limb exoskeleton toward tripping-free stair climbing," *ISA Transactions*, vol. 131, pp. 610–627, Dec. 2022.

[4] E. Trombin, S. Tortora, E. Menegatti, and L. Tonin, "Environment-Adaptive Gait Planning for Obstacle Avoidance in Lower-Limb Robotic Exoskeletons," in *2024 IEEE/RSJ International Conference on Intelligent Robots and Systems (IROS)*, pp. 13640–13647, Oct. 2024. ISSN: 2153-0866.

[5] O. N. Beck, M. K. Shepherd, R. Rastogi, G. Martino, L. H. Ting, and G. S. Sawicki, "Exoskeletons need to react faster than physiological responses to improve standing balance," *Science Robotics*, vol. 8, p. eadf1080, Feb. 2023.

[6] B. J. B. Lee, A. Williams, and P. Ben-Tzvi, "Intelligent Object Grasping With Sensor Fusion for Rehabilitation and Assistive Applications," *IEEE Transactions on Neural Systems and Rehabilitation Engineering*, vol. 26, pp. 1556–1565, Aug. 2018. Conference Name: IEEE Transactions on Neural Systems and Rehabilitation Engineering.

[7] T. du Plessis, K. Djouani, and C. Oosthuizen, "A Review of Active Hand Exoskeletons for Rehabilitation and Assistance," *Robotics*, vol. 10, p. 40, Mar. 2021. Number: 1 Publisher: Multidisciplinary Digital Publishing Institute.

[8] A. Zangrandi, M. D'Alonzo, C. Cipriani, and G. Di Pino, "Neurophysiology of slip sensation and grip reaction: insights for hand prosthesis control of slippage," *Journal of Neurophysiology*, vol. 126, pp. 477–492, Aug. 2021.

[9] M. A. Diftler, C. A. Ihrke, L. B. Bridgwater, J. M. Rogers, D. R. Davis, D. M. Linn, E. A. Laske, K. G. Ensley, and J. H. Lee, "Roboglove - a grasp assist device for earth and space," in *International Conference on Environmental Systems*, (Bellevue, WA), July 2015.

[10] D. Park, H. Kim, and C. C. Kemp, "Multimodal anomaly detection for assistive robots," *Autonomous Robots*, vol. 43, pp. 611–629, Mar. 2019.

[11] D. P. Losey, C. G. McDonald, E. Battaglia, and M. K. O'Malley, "A Review of Intent Detection, Arbitration, and Communication Aspects of Shared Control for Physical Human–Robot Interaction," *Applied Mechanics Reviews*, vol. 70, Feb. 2018.

[12] D. P. Losey and M. K. O'Malley, "Trajectory Deformations From Physical Human–Robot Interaction," *IEEE Transactions on Robotics*, vol. 34, pp. 126–138, Feb. 2018. Conference Name: IEEE Transactions on Robotics.

[13] B. Berberian, J.-C. Sarrazin, P. L. Blaye, and P. Haggard, "Automation Technology and Sense of Control: A Window on Human Agency," *PLOS ONE*, vol. 7, p. e34075, Mar. 2012. Publisher: Public Library of Science.

[14] T. Morita, Y. Zhu, T. Aoyama, M. Takeuchi, K. Yamamoto, and Y. Hasegawa, "Auditory Feedback for Enhanced Sense of Agency in Shared Control," *Sensors (Basel, Switzerland)*, vol. 22, p. 9779, Dec. 2022.

[15] B. Shneiderman and C. Plaisant, *Designing the user interface: strategies for effective human-computer interaction*. Boston: Pearson/Addison Wesley, 4th ed ed., 2004.

[16] B. Eitam, P. M. Kennedy, and E. Tory Higgins, "Motivation from control," *Experimental Brain Research*, vol. 229, pp. 475–484, Sept. 2013.

[17] G. Moretto, E. Walsh, and P. Haggard, "Experience of agency and sense of responsibility," *Consciousness and Cognition*, vol. 20, pp. 1847–1854, Dec. 2011.

[18] B. Berberian, "Man-Machine teaming: a problem of Agency," *IFAC-PapersOnLine*, vol. 51, pp. 118–123, Jan. 2019.

[19] K. O. Koerten, D. A. Abbink, and A. Zgonnikov, "Haptic Shared Control for Dissipating Phantom Traffic Jams," *IEEE Transactions on Human-Machine Systems*, vol. 54, pp. 11–20, Feb. 2024. Conference Name: IEEE Transactions on Human-Machine Systems.

[20] M. Pazzaglia and M. Molinari, "The embodiment of assistive devices—from wheelchair to exoskeleton," *Physics of Life Reviews*, vol. 16, pp. 163–175, Mar. 2016.

[21] D.-J. Kim, R. Hazlett-Knudsen, H. Culver-Godfrey, G. Rucks, T. Cunningham, D. Portee, J. Bricout, Z. Wang, and A. Behal, "How Autonomy Impacts Performance and Satisfaction: Results From a Study With Spinal Cord Injured Subjects Using an Assistive Robot," *IEEE Transactions on Systems, Man, and Cybernetics - Part A: Systems and Humans*, vol. 42, pp. 2–14, Jan. 2012. Conference Name: IEEE Transactions on Systems, Man, and Cybernetics - Part A: Systems and Humans.

[22] J. N. Wilkenfeld, S. Kim, S. Upasani, G. L. Kirkwood, N. E. Dunbar, and D. Srinivasan, "Sensemaking, adaptation and agency in human-exoskeleton synchrony," *Frontiers in Robotics and AI*, vol. 10, Oct. 2023. Publisher: Frontiers.

[23] M. Dufraisse, L. Wioland, J.-J. Atain-Kouadio, and J. Cegarra, "Occupational Exoskeletons as Symbionts: Defining Operator-Exoskeleton Interactions," in *Human Factors and Wearable Technologies*, vol. 141, AHFE Open Acces, 2024. ISSN: 27710718 Issue: 141.

[24] E. You and K. Hauser, "Assisted Teleoperation Strategies for Aggressively Controlling a Robot Arm with 2D Input," in *Robotics: Science and Systems VII*, Robotics: Science and Systems Foundation, June 2011.

[25] J. Baraglia, M. Cakmak, Y. Nagai, R. P. Rao, and M. Asada, "Efficient human-robot collaboration: When should a robot take initiative?," *The International Journal of Robotics Research*, vol. 36, pp. 563–579, June 2017. Publisher: SAGE Publications Ltd STM.

[26] Y. Zhang, V. Narayanan, T. Chakraborti, and S. Kambhampati, "A human factors analysis of proactive support in human-robot teaming," in *2015 IEEE/RSJ International Conference on Intelligent Robots and Systems (IROS)*, pp. 3586–3593, Sept. 2015.

[27] A. D. Dragan and S. S. Srinivasa, "A policy-blending formalism for shared control," *The International Journal of Robotics Research*, vol. 32, pp. 790–805, June 2013. Publisher: SAGE Publications Ltd STM.

[28] E. M. van Zoelen, E. I. Barakova, and M. Rauterberg, "Adaptive Leader-Follower Behavior in Human-Robot Collaboration," in *2020 29th IEEE International Conference on Robot and Human Interactive Communication (RO-MAN)*, pp. 1259–1265, Aug. 2020. ISSN: 1944-9437.

[29] N. Abe, Y. Hu, M. Benallegue, N. Yamanobe, G. Venture, and E. Yoshida, "Human Understanding and Perception of Unanticipated Robot Action in the Context of Physical Interaction," *J. Hum.-Robot Interact.*, vol. 13, pp. 9:1–9:26, Mar. 2024.

[30] M. A. Collier, R. Narayan, and H. Admoni, "The Sense of Agency in Assistive Robotics Using Shared Autonomy," Jan. 2025. arXiv:2501.07462 [cs].

[31] S. Massardi, D. Rodriguez-Cianca, D. Pinto-Fernandez, J. C. Moreno, M. Lancini, and D. Torricelli, "Characterization and Evaluation of Human–Exoskeleton Interaction Dynamics: A Review," *Sensors*, vol. 22, p. 3993, Jan. 2022. Number: 11 Publisher: Multidisciplinary Digital Publishing Institute.

[32] A. I. W. McPherson, V. V. Patel, P. R. Downey, A. Abbas Alvi, M. E. Abbott, and H. S. Stuart, "Motor-Augmented Wrist-Driven Orthosis: Flexible Grasp Assistance for People with Spinal Cord Injury," in *2020 42nd Annual International Conference of the IEEE Engineering in Medicine & Biology Society (EMBC)*, pp. 4936–4940, July 2020. ISSN: 2694-0604.

[33] W. D. A. Beggs and C. I. Howarth, "Movement Control in a Repetitive Motor Task," *Nature*, vol. 225, pp. 752–753, Feb. 1970. Publisher: Nature Publishing Group.

[34] S. G. Hart and L. E. Staveland, "Development of NASA-TLX (Task Load Index): Results of Empirical and Theoretical Research," in *Advances in Psychology* (P. A. Hancock and N. Meshkati, eds.), vol. 52 of *Human Mental Workload*, pp. 139–183, North-Holland, Jan. 1988.

[35] J. Pinheiro, D. Bates, and R Core Team, "nlme: Linear and nonlinear mixed effects models," manual, 2023. tex.howpublished: Online.

[36] D. Bates, M. Mächler, B. Bolker, and S. Walker, "Fitting Linear Mixed-Effects Models Using lme4," *Journal of Statistical Software*, vol. 67, pp. 1–48, Oct. 2015.

[37] R. V. Lenth, "Emmeans: Estimated marginal means, aka least-squares means," manual, 2024. tex.howpublished: Online.